NASA CONTRACTOR REPORT

NASA CR-296

NASA CR-296

FLEXURAL VIBRATIONS OF THE PRESTRESSED TOROIDAL SHELL

by Artis A. Liepins

Prepared under Contract No. NASw-955 *by*
DYNATECH CORPORATION
Cambridge, Mass.
for

NATIONAL AERONAUTICS AND SPACE ADMINISTRATION • WASHINGTON, D. C. • SEPTEMBER 1965

NASA CR-296

FLEXURAL VIBRATIONS OF THE PRESTRESSED TOROIDAL SHELL

By Artis A. Liepins

Prepared under Contract No. NASw-955 by
DYNATECH CORPORATION
Cambridge, Mass.

for

NATIONAL AERONAUTICS AND SPACE ADMINISTRATION

SUMMARY

Results of a numerical study of the natural frequencies and modes of vibration of the pressure prestressed toroidal shell are presented. The analysis is based upon a linearized theory of vibrations of prestressed shells. The frequencies and mode shapes are obtained by trial and error in the Holzer fashion. The effects of wall bending stiffness on the frequencies of shells under varying degrees of prestress are shown.

A

ALT. R. HS

end

to p. 19

CONTENTS

ILLUSTRATIONS

Figure

NOMENCLATURE

a_m, b_m	amplitudes of ring flexural vibrations
h	thickness of shell
k	$(1 - \nu^2)\,\kappa$
p	pressure
q_α	DQ_α/R^2
r	$(1 - \epsilon \cos \alpha)/\epsilon$
u	meridional displacement (Figure 1)
v	circumferential displacement (Figure 1)
w	normal displacement (Figure 1)
C, N, Q, S $T_0, T_1, T_2 \ldots T_{12}$	defined functions
D	$Eh^3/12\,(1 - \nu^2)$
E	Young's modulus
E_α, E_θ, $E_{\alpha\theta}$	membrane strains
M_α, M_θ, $M_{\alpha\theta}$	stress couples
N_α, N_θ, $N_{\alpha\theta}$	stress resultants
Q_α, Q_θ	transverse shear stress resultants
R	radius of the generating circle of torus (Figure 1)
S_α, S_θ	membrane prestress forces
α	meridional position angle (Figure 1)
ϵ	ratio of the two radii of the torus (Figure 1)

θ	circumferential position angle (Figure 1)
κ	pR/Eh, prestress parameter
κ_α, κ_θ, $\kappa_{\alpha\theta}$	bending strains
λ	$(\rho R^2/E\epsilon^2)\,\omega^2$, frequency parameter
ν	Poisson's ratio
ρ	material density
ϕ_α, ϕ_θ, $\phi_{\alpha\theta}$	rotations of the normal to the shell
ω	circular frequency
Γ	$(h/R)^2/12$
Δ	spacing between finite difference stations

Matrices

a, b, c	5 x 5 matrices
x	1 x 5 column matrix
A, B, C, D, E, F, G, H, P	4 x 4 matrices
$\bar{A}$, $\bar{B}$, $\bar{C}$	3 x 3 matrices
Z	1 x 4 column matrix
$\bar{Z}$	1 x 3 column matrix

Indices

i	station
I	last station
m	Fourier index of ring flexural vibrations
n	Fourier index of shell vibrations

Section 1
INTRODUCTION

A study of the free vibrations of the pressure prestressed toroidal membrane [1] shows that the frequencies can be grouped into four families: a family of flexural vibrations associated with relatively low frequencies, and three families of vibrations with high frequencies. The flexural vibrations are found to depend strongly on prestress. The vibrations of the other three families are practically insensitive to prestress. Since both the effects of prestress and the effects of wall bending stiffness enter the fundamental equations in a similar manner (through terms whose coefficients are small compared to the coefficients associated with the membrane terms), it can be expected that bending stiffness has a strong influence on the frequencies of the flexural vibrations. This report presents the results of a numerical study of the effect of wall bending stiffness on the frequencies and mode shapes of the flexural vibrations.

Several iterative numerical methods suitable for the analysis of the free vibrations of shells of revolution have appeared recently in the literature [1] [2] [3]. Kalnins [2] uses a multisegment direct numerical integration approach and Reference [1] uses finite differences to evaluate a certain determinant corresponding to a trial value of the frequency. Cohen [3] uses a method which iterates on the mode shape instead of the frequency. Although the methods of References [2] and [3] are applied to shells of revolution without prestress, their extension to shells with prestress appears to be straightforward. None of these methods, however, possesses a substantial advantage over the others. This study uses the numerical method of Reference [1].

Section 2
FUNDAMENTAL EQUATIONS

The present analysis of the free vibrations of the pressure prestressed toroidal shell is based upon a set of equations which result from the addition of the bending terms of the Sanders linear shell theory [4] to the prestressed membrane equations presented in Reference [1]. These are (refer to Figure 1):

Equilibrium

$$\frac{\partial}{\partial \alpha}(rN_\alpha) + \frac{\partial N_{\alpha\theta}}{\partial \theta} - N_\theta \sin\alpha + rQ_\alpha + \frac{1}{2R}\left(1 + \frac{\cos\alpha}{r}\right)\frac{\partial}{\partial \theta}(M_{\alpha\theta})$$
$$+ S_\theta\left[\frac{\partial}{\partial \theta}(E_{\alpha\theta} - \phi_{\alpha\theta}) + (E_\alpha - E_\theta)\sin\alpha\right] + rS_\alpha\left(\frac{\partial E_\alpha}{\partial \alpha} - \phi_\alpha\right)$$
$$+ pRr\,\phi_\alpha + \rho h R\omega^2 ru = 0 \tag{1}$$

$$\frac{\partial N_\theta}{\partial \theta} + \frac{\partial}{\partial \alpha}(rN_{\alpha\theta}) + N_{\alpha\theta}\sin\alpha - Q_\theta\cos\alpha - \frac{r}{2R}\frac{\partial}{\partial \alpha}\left[\left(1 + \frac{\cos\alpha}{r}\right)M_{\alpha\theta}\right]$$
$$+ S_\theta\left[\frac{\partial E_\theta}{\partial \theta} + 2E_{\alpha\theta}\sin\alpha + \phi_\theta\cos\alpha\right] + rS_\alpha\frac{\partial}{\partial \alpha}(E_{\alpha\theta} + \phi_{\alpha\theta})$$
$$+ pRr\,\phi_\theta + \rho h R\omega^2 rv = 0 \tag{2}$$

$$rN_\alpha - N_\theta\cos\alpha - \frac{\partial}{\partial \alpha}(rQ_\alpha) - \frac{\partial Q_\theta}{\partial \theta} + S_\theta\left[\frac{\partial \phi_\theta}{\partial \theta} + \phi_\alpha\sin\alpha - E_\theta\cos\alpha\right]$$
$$+ rS_\alpha\left(\frac{\partial \phi_\alpha}{\partial \alpha} + E_\alpha\right) - pRr(E_\alpha + E_\theta) - \rho h R\omega^2 rw = 0 \tag{3}$$

$$\frac{\partial}{\partial \alpha}(rM_\alpha) + \frac{\partial M_{\alpha\theta}}{\partial \theta} - M_\theta\sin\alpha - RrQ_\alpha = 0 \tag{4}$$

$$\frac{\partial M_\theta}{\partial \theta} + \frac{\partial}{\partial \alpha}(rM_{\alpha\theta}) + N_{\alpha\theta}\sin\alpha - RrQ_\theta = 0 \tag{5}$$

Strain Displacement

$$RE_\alpha = \frac{\partial u}{\partial \alpha} + w \tag{6}$$

$$rRE_\theta = \frac{\partial v}{\partial \theta} + u \sin\alpha - w\cos\alpha \tag{7}$$

$$2rRE_{\alpha\theta} = r\frac{\partial v}{\partial \alpha} + \frac{\partial u}{\partial \theta} - v\sin\alpha \tag{8}$$

$$R\kappa_\alpha = \frac{\partial \phi_\alpha}{\partial \alpha} \tag{9}$$

$$rR\kappa_\theta = \frac{\partial \phi_\theta}{\partial \theta} + \phi_\alpha \sin\alpha \tag{10}$$

$$2rR\kappa_{\alpha\theta} = r\frac{\partial \phi_\theta}{\partial \alpha} + \frac{\partial \phi_\alpha}{\partial \theta} - \phi_\theta \sin\alpha - (r + \cos\alpha)\phi_{\alpha\theta} \tag{11}$$

$$R\phi_\alpha = -\frac{\partial w}{\partial \alpha} + u \tag{12}$$

$$-rR\phi_\theta = \frac{\partial w}{\partial \theta} + v\cos\alpha \tag{13}$$

$$-2rR\phi_{\alpha\theta} = \frac{\partial u}{\partial \theta} - \frac{\partial}{\partial \alpha}(rv) \tag{14}$$

Constitutive Relations

$$EhE_\alpha = N_\alpha - \nu N_\theta \tag{15}$$

$$EhE_\theta = N_\theta - \nu N_\alpha \tag{16}$$

$$EhE_{\alpha\theta} = (1+\nu)N_{\alpha\theta} \tag{17}$$

$$\frac{Eh^3}{12}\kappa_\alpha = M_\alpha - \nu M_\theta \tag{18}$$

$$\frac{Eh^3}{12}\kappa_\theta = M_\theta - \nu M_\alpha \tag{19}$$

$$\frac{Eh^3}{12}\kappa_{\alpha\theta} = (1+\nu)M_{\alpha\theta} \tag{20}$$

The above constitute twenty equations for the twenty unknowns N_α, N_θ, $N_{\alpha\theta}$, E_α, E_θ, $E_{\alpha\theta}$, M_α, M_θ, $M_{\alpha\theta}$, κ_α, κ_θ, $\kappa_{\alpha\theta}$, Q_α, Q_θ, ϕ_α, ϕ_θ, $\phi_{\alpha\theta}$, u, v, and w. The stress resultants S_α and S_θ are known functions of prestress.

The state of prestress is determined from a separate analysis of the toroidal shell subjected to static internal pressure. An analysis based on the linear membrane theory [5] gives

$$
\begin{aligned}
S_\alpha &= pR \, \frac{1 - \frac{1}{2}\epsilon \cos\alpha}{1 - \epsilon \cos\alpha} \\
S_\theta &= \frac{1}{2} pR
\end{aligned}
\tag{21}
$$

Analyses of the toroidal membrane under internal pressure based upon nonlinear theories [6, 7] show that the linear meridional stress resultant, S_α, is in error by a negligible amount, but that the linear circumferential stress resultant, S_θ, can be in error by 18%. The significant difference, however, between the linear and nonlinear stress distributions is confined to a small area of the torus at $\alpha = \pm \pi/2$. Furthermore, an analysis [8] of the toroidal shell under internal pressure based upon equations which consider wall bending stiffness and nonlinear behavior shows that the stress resultants do not differ substantially from those obtained from nonlinear membrane theory. Hence, it appears that the state of prestress determined according to the linear membrane theory is adequately accurate for the present analysis of vibrations.

Section 3
REDUCTION TO SECOND ORDER DIFFERENTIAL EQUATIONS

The solution of the fundamental equations (1-20) is started by separating the variables. Set

$$\begin{bmatrix} N_\alpha, E_\alpha, M_\alpha, \kappa_\alpha, \phi_\alpha, u \\ N_\theta, E_\theta, M_\theta, \kappa_\theta, Q_\alpha, w \end{bmatrix} = \begin{bmatrix} N_{\alpha n}, E_{\alpha n}, M_{\alpha n}, \kappa_{\alpha n}, \phi_{\alpha n}, & Ru_n \\ N_{\theta n}, E_{\theta n}, M_{\theta n}, \kappa_{\theta n}, \frac{D}{R^2} q_{\alpha n}, & Rw_n \end{bmatrix} \cos n\theta$$

$$\begin{bmatrix} N_{\alpha\theta}, E_{\alpha\theta}, \phi_\theta, \phi_{\alpha\theta} \\ M_{\alpha\theta}, \kappa_{\alpha\theta}, Q_\theta, v \end{bmatrix} = \begin{bmatrix} N_{\alpha\theta n}, E_{\alpha\theta n}, \phi_{\theta n}, \phi_{\alpha\theta n} \\ M_{\alpha\theta n}, \kappa_{\alpha\theta n}, Q_{\theta n}, Rv_n \end{bmatrix} \sin n\theta \tag{22}$$

Next, define

$$\begin{aligned} S &= (\sin\alpha)/r \\ C &= (\cos\alpha)/r \\ N &= n/r \end{aligned} \tag{23}$$

Then, use of equations (22) and (23) in equations (1-14) yields

$$\begin{aligned} &N_\alpha' + S(N_\alpha - N_\theta) + NN_{\alpha\theta} + \frac{D}{R^2} q_\alpha + \frac{N}{2R}(1+C) M_{\alpha\theta} \\ &+ S_\theta [N(E_{\alpha\theta} - \phi_{\alpha\theta}) + S(E_\alpha - E_\theta)] + S_\alpha (E_\alpha' - \phi_\alpha) \\ &+ pR\phi_\alpha + \rho h R^2 \omega^2 u = 0 \end{aligned} \tag{24}$$

$$\begin{aligned} &N_{\alpha\theta}' + 2SN_{\alpha\theta} - NN_\theta - CQ_\theta - \frac{1}{2R}(1+C)(M_{\alpha\theta}' - SM_{\alpha\theta}) \\ &+ S_\theta(-NE_\theta + 2SE_{\alpha\theta} + C\phi_\theta) + S_\alpha(E_{\alpha\theta}' + \phi_{\alpha\theta}') \\ &+ pR\phi_\theta + \rho h R^2 \omega^2 v = 0 \end{aligned} \tag{25}$$

$$N_\alpha - CN_\theta - \frac{D}{R^2}(q_\alpha' + Sq_\alpha) - NQ_\theta + S_\theta(N\phi_\theta + S\phi_\alpha - CE_\theta)$$

$$+ S_\alpha(\phi_\alpha' + E_\alpha) - pR(E_\alpha + E_\theta) - \rho h R^2 \omega^2 w = 0 \tag{26}$$

$$M_\alpha' + S(M_\alpha - M_\theta) + NM_{\alpha\theta} - \frac{D}{R} q_\alpha = 0 \tag{27}$$

$$M_{\alpha\theta}' + 2SM_{\alpha\theta} - NM_\theta - RQ_\theta = 0 \tag{28}$$

$$E_\alpha = u' + w \tag{29}$$

$$E_\theta = Nv + Su - Cw \tag{30}$$

$$2E_{\alpha\theta} = v' - Sv - Nu \tag{31}$$

$$R\kappa_\alpha = \phi_\alpha' \tag{32}$$

$$R\kappa_\theta = S\phi_\alpha + N\phi_\theta \tag{33}$$

$$2R\kappa_{\alpha\theta} = \phi_\theta' - S\phi_\theta - N\phi_\alpha - (1+C)\phi_{\alpha\theta} \tag{34}$$

$$\phi_\alpha = -w' + u \tag{35}$$

$$\phi_\theta = Nw - Cv \tag{36}$$

$$2\phi_{\alpha\theta} = Nu + v' + Sv \tag{37}$$

In equations (24-37) and subsequent expressions the subscript n has been dropped. Prime indicates differentiation with respect to α.

At this point the problem has been reduced to the simultaneous solution of the ordinary differential equations (24-37) and (15-20). Our goal is to derive four simultaneous second order differential equations for u, v, ϕ_α, and q_α. First eliminate Q_θ from equations (25) and (26) using equation (28). Then, substitute the strain displacement relations (29-34), two of the rotation expressions (36, 37), and the constitutive relations (15-20) into the equilibrium equations (24-27). The resulting equations together with (35) constitute five equations for u, v, w, ϕ_α, and q_α. They may be written in matrix form as

$$ax'' + bx' + c\,x = 0 \qquad (38a, b, c, d, e)$$

where

$$x = \begin{Bmatrix} u \\ v \\ w \\ \phi_\alpha \\ q_\alpha \end{Bmatrix}$$

The elements of the a, b, c matrices are given in Appendix A.

We now manipulate equations (38) so that w can be eliminated using equation (38c) (equilibrium of forces in the normal direction). In order that no derivatives higher than the second derivative appear in the final equations, eliminate v'' from equation (38c) using equation (38b) (equilibrium of forces in the circumferential directions) as follows:

$$v'' = \frac{1}{a_{22}}(b_{21}u' + c_{21}u + b_{22}v' + c_{22}v + a_{23}w'' + b_{23}w' + c_{23}w + b_{24}\phi_\alpha' + c_{24}\phi_\alpha) \qquad (39)$$

Then equation (38c) reads:

$$\bar{b}_{31}u' + \bar{c}_{31}u + \bar{b}_{32}v' + \bar{c}_{32}v + \bar{a}_{33}w'' + \bar{b}_{33}w' + \bar{c}_{33}w + \bar{b}_{34}\phi_\alpha' + \bar{c}_{34}\phi_\alpha - \Gamma q_\alpha' - \Gamma S q_\alpha = 0 \qquad (40)$$

where the coefficients are given in the appendix. From equation (35)

$$\begin{aligned} w' &= u - \phi_\alpha \\ w'' &= u' - \phi_\alpha' \end{aligned} \qquad (41)$$

After eliminating the derivatives of w using (41), equation (40) can be written as

$$Qw = T_1u' + T_2u + T_3v' + T_4v + T_5\phi_\alpha' + T_6\phi_\alpha - \Gamma q_\alpha' - \Gamma S q_\alpha \qquad (42)$$

and the derivative of w can be written as

$$Qw' = T_1 u'' + (T_1' + T_2)\, u' + T_2' u + T_3 v'' + (T_3' + T_4)\, v' + T_4'\, v$$
$$+ T_5 \phi_\alpha'' + (T_5' + T_6)\, \phi_\alpha' + T_6' \phi_\alpha - \Gamma q_\alpha'' - \Gamma S q_\alpha' - \Gamma (C - S^2)\, q_\alpha - Q' w \tag{43}$$

The T' s and Q are defined in the appendix.

Now, multiply equations (38a, b, d, e) by Q and eliminate Qw' from them with equation (43). Then multiply the resulting equations by Q and eliminate Qw with equation (42). The resulting four equations for u, v, ϕ_α, and q_α may be written in matrix form as

$$AZ'' + BZ' + CZ = 0 \tag{44}$$

where

$$Z = \begin{Bmatrix} u \\ v \\ \phi_\alpha \\ q_\alpha \end{Bmatrix}$$

and the elements of A, B, and C are given in Appendix A.

The basic equations (44) simplify for the case of axisymmetric vibrations, n = 0, v = 0. The equation of equilibrium of forces in the circumferential direction is then satisfied identically, and equations (44) become

$$\overline{A}\overline{Z}'' + \overline{B}\overline{Z}' + \overline{C}\overline{Z} = 0 \tag{45}$$

where

$$\overline{Z} = \begin{Bmatrix} u \\ \phi_\alpha \\ q_\alpha \end{Bmatrix}$$

The elements of $\overline{A}$, $\overline{B}$, and $\overline{C}$ are the remaining elements of A, B, and C if the second row and column are deleted, and N is set equal to zero.

The fundamental equations have now been reduced to the solution of two sets of second order differential equations as follows: 1) four equations (44) for the general case, 2) three equations (45) for the axisymmetric case. These differential equations will be integrated numerically by a method described in Reference [1]. For completeness, the description of the numerical method is reproduced in the next section.

At this point we remark that the fundamental equations (1-20) could be more easily reduced to four second order differential equations for u, v, w, and M_α in the manner of Budiansky and Radkowski [9]. However, application of the numerical method described in the next section resulted in a convergence of the finite differences which was too slow for practical computation.

The fundamental equations can also be reduced to four equations for v, w, N_α, and M_α. First, derive a set of five equations for u, v, w, N_α and M_α, then solve the equation of equilibrium of forces in the meridional direction for u, and finally eliminate u from the remaining four equations. The application of the present numerical analysis to these equations resulted in efficient and accurate results except in the approximate range

$$\frac{n^2}{2\,(1+\nu)(1+\epsilon)^2} < \lambda < \frac{n^2}{2\,(1+\nu)(1-\epsilon)^2}$$

In this range the coefficient of u in the equation of equilibrium of forces in the meridional direction has a zero.

Section 4
NUMERICAL ANALYSIS

Since the geometry and prestress are symmetrical about $\alpha = 0$ and $\alpha = \pi$, we need to consider only one-half of the torus corresponding to the range $0 \leq \alpha \leq \pi$. Let this range be subdivided by I + 1 equally spaced stations. Then the spacing between stations is

$$\Delta = \pi / I$$

and the position angle for the i^{th} station is

$$\alpha_i = i \Delta \qquad i = 0, 1, 2, \ldots\ldots I$$

The derivatives of Z at the i^{th} station are approximated by the central difference formulas

$$Z_i' = \frac{1}{2\Delta} (Z_{i+1} - Z_{i-1})$$

$$Z_i'' = \frac{1}{\Delta^2} (Z_{i+1} - 2Z_i + Z_{i-1}) \qquad (46)$$

With these formulas we obtain from equation (44) the set of difference equations

$$D_i Z_{i+1} + E_i Z_i + F_i Z_{i-1} = 0 \qquad (47)$$

$$i = 0, 1, 2, \ldots\ldots I$$

where

$$D_i = \frac{2}{\Delta} A_i + B_i$$

$$E_i = -\frac{4}{\Delta} A_i + 2\Delta C_i$$

$$F_i = \frac{2}{\Delta} A_i - B_i \qquad (48)$$

The difference equations (47) are augmented by conditions at $i = 0$ and $i = I$. These end conditions are obtained from considerations of continuity of the displacement functions, u, v, and w. Now, the solution of the fundamental equations (1-20), and the reduced equations (44) are such that either v and w are even, u is odd or v and w are odd, and u is an even function of α with respect to $\alpha = 0$ and π. These two groups of solutions will be denoted as symmetric and antisymmetric modes respectively. Hence, the end conditions are

$$\begin{aligned} Z_{-1} &= \pm GZ_1 \\ Z_{I+1} &= \pm GZ_{I-1} \end{aligned} \tag{49}$$

where G is the diagonal matrix

$$G = \begin{bmatrix} -1 & & & \\ & 1 & & \\ & & -1 & \\ & & & -1 \end{bmatrix}$$

and plus and minus signs refer to symmetric and antisymmetric modes respectively.

The difference equations (47) together with the end conditions (49) make up a set of homogeneous algebraic equations. The eigenvalues of these equations are obtained by trial and error, using a special Gaussian elimination technique devised by Potters [10].

The equations for this procedure are obtained as follows. Let

$$Z_i = - P_i Z_{i+1} \tag{50}$$

Substitute this expression into the difference equations (47), and by comparing the result with (50) obtain the recurrence relation

$$P_i = [E_i - F_i P_{i-1}]^{-1} D_i$$

$$i = 1, 2, 3, \ldots\ldots I-1 \tag{51}$$

Now, write the difference equations (47) at $i = 0$ and eliminate Z_{-1} using the first of the end conditions (49). Again, by comparing the result with equation (50) obtain

$$P_0 = E_0^{-1} [D_0 \pm F_0 G] \tag{52}$$

where plus and minus signs refer to symmetric and antisymmetric modes respectively. Equations (52) together with the recurrence relation (51) provide all the P's up to P_{I-1}. Finally, write the difference equations (47) at $i = I$. Eliminate Z_{I+1} using the second of the end conditions (49), and Z_{I-1} using equation (50). The result is

$$[E_I - (F_I \pm D_I G) P_{I-1}] Z_I = H Z_I = 0 \tag{53}$$

Since $Z_I \neq 0$, we must require that the determinant

$$\nabla = \left| E_I - (F_I \pm D_I G) P_{I-1} \right| \tag{54}$$

vanish. Equation (54) is effectively a frequency equation. A value of λ which gives $\nabla = 0$ is a natural frequency of vibration.

The mode shape corresponding to a natural frequency can be calculated once a λ for which $\nabla = 0$ is obtained. Set the amplitude of one of the displacements at $i = I$ equal to unity and calculate the remaining unknowns at $i = I$ from three of the equations (53). Thus, for the symmetric modes

$$Z_I = \begin{Bmatrix} 0 \\ 1 \\ 0 \\ 0 \end{Bmatrix} \tag{55}$$

For antisymmetric modes

$$Z_I = \begin{Bmatrix} 1 \\ 0 \\ \phi_{\alpha I} \\ q_{\alpha I} \end{Bmatrix} \tag{56}$$

where

$$\begin{Bmatrix} \phi_{\alpha I} \\ q_{\alpha I} \end{Bmatrix} = - \begin{bmatrix} H_{33} & H_{34} \\ H_{43} & H_{44} \end{bmatrix}^{-1} \begin{Bmatrix} H_{31} \\ H_{41} \end{Bmatrix} \tag{57}$$

The remaining Z's can then be calculated from equations (50) in the reverse order.

The w displacement is obtained from equation (42). In finite difference form the equation reads

$$\begin{aligned} w_i = \frac{1}{Q_i} \Big\{ & \frac{1}{2\Delta} [T_{1,i} (Z_{1,i+1} - Z_{1,i-1}) + T_{3,i} (Z_{2,i+1} - Z_{2,i-1}) \\ & + T_{5,i} (Z_{3,i+1} - Z_{3,i-1}) - \Gamma (Z_{4,i+1} - Z_{4,i-1})] \\ & + T_{2,i} Z_{1,i} + T_{4,i} Z_{2,i} + T_6 Z_{3,i} - \Gamma S_i Z_{4,i} \Big\} \\ & \qquad i = 1, 2, 3, \ldots\ldots I-1 \end{aligned} \tag{58}$$

For symmetrical mode shapes

$$\begin{aligned} w_0 &= \frac{1}{Q_0} [\frac{1}{\Delta} (T_{1,0} Z_{1,1} + T_{5,0} Z_{3,1} - \Gamma Z_{4,1}) + T_{4,0} Z_{2,0}] \\ w_I &= \frac{1}{Q_I} [\frac{-1}{\Delta} (T_{1,I} Z_{1,I-1} + T_{5,I} Z_{3,I-1} - \Gamma Z_{4,I-1}) + T_{4,0}] \end{aligned} \tag{59}$$

and for antisymmetrical mode shapes

$$w_0 = w_I = 0 \tag{60}$$

The procedure may be summarized as follows:

1. Assume a value of λ;
2. Calculate the elements of the A, B, C, D, E, F, and P matrices at all stations from equations (44), (48), (51) and (52);
3. Calculate the determinant ∇ from equation (54);

4. Repeat steps 1-3 and plot ∇ versus λ. From this plot determine a λ for which $\nabla = 0$. This λ is a natural frequency;

5. Calculate the mode shape corresponding to a natural frequency from equations (50) and (55-60).

The equations in this procedure were programmed for the IBM 7094 computer.

A number of natural frequencies were calculated with $I = 50$ and 100 and compared. The difference was found to be less than one percent. Therefore, all results were obtained with $I = 50$. For this number of finite difference spacings the IBM 7094 required approximately 1.5 seconds to evaluate one determinant ∇ of the general vibrations.

Section 5
RESULTS

Results of the present numerical analysis are contained in Figures 2-20. These results show the effect of bending stiffness on the vibration of shells under 1) high prestress, $\kappa = 0.002$, 2) low prestress, $\kappa = 0.0001$, and 3) no prestress, $\kappa = 0$. All results are for Poisson's ratio $\nu = 0.3$.

The modes of the flexural vibrations of the prestressed toroidal shell may be thought to consist of two types of vibrations: 1) the modes of a torus whose meridional curve (cross-section) is not allowed to distort (overall ring vibrations), 2) the modes of a pressure prestressed circular ring with radius R (cross-sectional or ring flexural vibrations). The first type is approximated by the vibrations of a thin ring of radius R/ϵ without prestress [11]:

Bending modes

symmetric (in plane bending)

$$\lambda = \epsilon^2 \frac{n^2 (n^2 - 1)^2}{2 (n^2 + 1)} \tag{61}$$

antisymmetric (out of plane bending)

$$\lambda = \epsilon^2 \frac{n^2 (n^2 - 1)^2}{2 (n^2 + 1 + \nu)} \tag{62}$$

Extensional modes (symmetric)

$$\lambda = n^2 + 1 \tag{63}$$

Torsional modes (antisymmetric)

$$\lambda = \frac{1}{2} (1 + \frac{n^2}{1 + \nu}) \tag{64}$$

The frequencies of flexural vibrations of a pressure prestressed ring of radius R are derived in Appendix B:

$$\lambda = \frac{1}{\epsilon^2} \frac{m^2(m^2-1)}{m^2+1} [\kappa + \Gamma (m^2-1)] \tag{65}$$

The effect of bending stiffness on the frequencies of a shell with high prestress are shown in Figures 2-7. These results are for n = 0, 1, and 2, $\kappa = 0.002$ and $h/R = 0.01$. It can be seen that the frequencies of the first mode of each type of vibration shown are practically unaffected by bending. However, the effect of bending increases with the mode number so that the increase in frequency of the fourth mode is of the order of 10%. This trend is forecast by the frequencies of the uncoupled ring flexural vibrations given by equation (65) in which the Γ part increases with $(m^2 - 1)$. The effect of bending is larger on shells with high ϵ (fat toroids). This is also to be expected because for high ϵ the mode shapes consist mostly of local deformation of the meridional curve [1]. For $\epsilon = 0.75$, n = 0 symmetric vibrations, the mode shapes of the first four modes of a shell with and without bending are compared in Figure 8. This figure shows that the effect of bending on these mode shapes is small. In summary, we can say that for shells with $\kappa = 0.002$ and $h/R = 0.01$ the effect of bending on the first four modes of the n = 0, 1, 2 vibrations is only moderate.

The effect of bending on the axisymmetric, symmetric, frequencies of a shell with $\kappa = 0.0001$ and $h/R = 0.01$ is shown in Figure 9. In this case, bending has increased the frequencies by approximately a factor of two when $\epsilon = 0.75$. For smaller ϵ the increase is smaller. For a shell with $\kappa = 0.0001$ and $h/R = 0.001$ the frequencies increase by less than 5%.

Frequency curves for a shell without prestress, $\kappa = 0$, n = 0 and 2 and $h/R = 0.01$ are shown in Figures 10-13. The dashed curves in these figures represent the frequencies of the uncoupled modes. The shell frequency curves are the solid curves. These curves exhibit transition regions which occur as sharp jumps for the axisymmetric, symmetric, frequency curve, and as more gradual changes for the axisymmetric, antisymmetric, and $n = 2$ frequency curves. In a qualitative sense these frequency curves exhibit the same features as those of the prestressed membrane when $\kappa = 0.002$ [1] (or refer to the dashed curves of Figures 2-7 of this report).

The axisymmetric mode shapes for a shell without prestress, $\kappa = 0$, and $h/R = 0.01$ are shown in Figures 14 and 15. The first column of mode shapes in these figures shows essentially the uncoupled mode shapes for ϵ below the transition region. In this region the overall ring mode shape prevails for the symmetric vibrations, but for the antisymmetric vibrations an irregular shape appears. The third column again shows essentially the uncoupled mode shapes. These are for ϵ above the transition region and are one order of complexity higher than those below the transition region. The fourth column shows mode shapes for $\epsilon = 0.75$ which are predominantly local oscillations of the meridional curve. In a qualitative sense, the mode shapes of the shell without prestress and $h/R = 0.01$ exhibit the same features as those of the prestressed membrane when $\kappa = 0.002$ [1].

Frequency curves for a shell without prestress, $\kappa = 0$, $n = 0$ and 2 and $h/R = 0.001$ are shown in Figures 16-19. The significant feature of these curves is their tendency to pair up with nearly the same frequencies. Examples of the mode shapes, shown in Figure 20, associated with frequencies that pair up appear to be mirror images of each other. That is, if the mode shape of the second symmetric mode is folded on top of the mode shape of the first symmetric mode, then the two mode shapes are nearly the same. The third and fourth symmetric, second and third antisymmetric and fourth and fifth antisymmetric mode shapes shown in Figure 20 are mirror images also. Another significant feature of the mode shapes presented in Figure 20, is the fact that the motion takes place mainly near the crowns.

The paired up frequencies with nearly the same mode shapes can be explained by the following. Let the radius of the torus go to infinity ($\epsilon \to 0$). Then the torus approaches a cylindrical shell. At every natural frequency of the cylindrical shell there are actually two identical frequencies with identical mode shapes. These frequencies separate slightly and the mode shapes become slightly different when imperfections (for example, when the cylindrical shell is not exactly circular) are present. Thus the pairing up of the frequencies of the toroidal shell are due to the weak influence of the circumferential curvature which has the equivalent effect of imperfections on the frequencies of the cylindrical shell.

Section 6
CONCLUSIONS

The following conclusions are drawn from this study:

1) Bending stiffness has only a moderate effect on the natural frequencies and mode shapes of relatively thick shells, ($^h/_R$ = 0.01) under high prestress (κ = 0.002).

2) When prestress is small (κ = 0.0001) bending stiffness increases the natural frequencies of relatively thick and fat toroidal shells (ϵ large, $^h/_R$ = 0.01) by as much as a factor of two.

3) In the absence of prestress, when membrane theory predicts a continuous frequency spectrum with discontinuous mode shapes, the consideration of bending stiffness leads to discrete frequencies with continuous mode shapes.

4) Bending stiffness should be considered in the calculation of the natural frequencies and mode shapes associated with the flexural vibrations of toroidal shells. end

Section 7

REFERENCES

1. Liepins, A. A., "Free Vibrations of the Prestressed Toroidal Membrane," AIAA Paper 65-110 (1965)

2. Kalnins, A., "Free Vibration of Rotationally Symmetric Shells," J. Acoust. Soc. Am., Vol. 36, No. 7, pp. 1355-1365 (1964)

3. Cohen, G. A., "Computer Analysis of Asymmetric Free Vibrations of Orthotropic Shells of Revolution," AIAA Paper 65-109 (1965)

4. Sanders, J. L., Jr., "An Improved First-Approximation Theory for Thin Shells," NASA TR R-24 (1959)

5. Timoshenko, S., "Theory of Plates and Shells" (McGraw-Hill Book Co., Inc., New York, 1940) Chapter X

6. Jordan, P. F., "Stresses and Deformations of the Thin-Walled Pressurized Torus" J. Aerospace Sci. 29, 213-225, (1962)

7. Sanders, J. L., Jr., and A. A. Liepins, "Toroidal Membrane Under Internal Pressure," AIAA Journal, Vol. 1, No. 9, 2105-2110 (1963)

8. Rosettos, J. N., and J. L. Sanders, Jr., "Toroidal Shells Under Internal Pressure in the Transition Range," AIAA Paper 65-145 (1965)

9. Budiansky, B., and P. P. Radkowski, "Numerical Analysis of Unsymmetrical Bending of Shells of Revolution," AIAA Journal, 1 (8), 1833-1842 (1963)

10. Potters, M. L., "A Matrix Method for the Solution of a Second Order Difference Equation in Two Variables," Math. Centrum Report MR 19 (1955)

11. Love, A. E. H., "The Mathematical Theory of Elasticity," (Dover Publications, New York, 1927).

APPENDIX A

Elements of Matrices

The non zero elements of the a, b, and c matrices are:

$$a_{11} = 1 + k\,(1 + \tfrac{1}{2}C)$$

$$a_{22} = \tfrac{1}{2}(1 - \nu) + k\,(1 + \tfrac{1}{2}C) + \tfrac{1}{8}(1 - \nu)\;\Gamma\;(1 + 3C)^2$$

$$a_{23} = -\tfrac{1}{4}(1 - \nu)\;\Gamma(1 + 3C)\,N = -\,a_{32}$$

$$a_{33} = -\tfrac{1}{2}(1 - \nu)\;\Gamma N^2$$

$$a_{54} = 1$$

$$b_{11} = (1 + \tfrac{1}{2}k)\,S$$

$$b_{12} = N\,[\,\tfrac{1}{2}(1 - \nu) - \tfrac{1}{8}(1 - \nu)\;\Gamma\,(1 + C)\,(1 + 3C)\,] = -\,b_{21}$$

$$b_{13} = 1 - \nu C + k\,(1 + \tfrac{1}{2}C) + \tfrac{1}{4}(1 - \nu)\;\Gamma\,(1 + C)\,N^2$$

$$b_{22} = \tfrac{1}{2}S\,[\,1 - \nu + k - \tfrac{1}{4}(1 - \nu)\;\Gamma\,(1 + 3C)\,(5 + 3C)\,]$$

$$b_{23} = \tfrac{1}{2}(1 - \nu)\;\Gamma N S\,(2 + 3C)$$

$$b_{24} = \Gamma N\,[\,\nu C + \tfrac{1}{4}(1 - \nu)\,(1 + 3C)\,] = -\;\Gamma\,b_{52}$$

$$b_{31} = 1 - \nu C + \tfrac{1}{2}kC + \tfrac{1}{4}(1 - \nu)\;\Gamma\,(1 + C)\,N^2$$

$$b_{32} = -\tfrac{1}{2}(1 - \nu)\;\Gamma N S$$

$$b_{33} = \tfrac{1}{2}(1 - \nu)\;\Gamma N^2 S$$

$$b_{34} = k\,(1 + \tfrac{1}{2}C) + \tfrac{1}{2}(1 + \nu)\;\Gamma N^2$$

$$b_{35} = -\Gamma$$

$$b_{43} = 1$$

$$b_{53} = \frac{1}{2}(1+\nu)\,N^2$$

$$b_{54} = S$$

$$c_{11} = (1-\nu^2)\,\epsilon^2\lambda + \nu C - S^2 - \frac{1}{2}(1-\nu)N^2 - \frac{1}{2}k\,(N^2+S^2) - \frac{1}{8}(1-\nu)\Gamma\,(1+C)^2 N^2$$

$$c_{12} = NS\,[-\frac{1}{2}(3-\nu) - k + \frac{1}{8}(1-\nu)\,\Gamma\,(1+C)\,(1+3C)]$$

$$c_{13} = S\,(1+C)\,[1+\frac{1}{2}k - \frac{1}{2}(1-\nu)\,\Gamma\,N^2]$$

$$c_{14} = -\frac{1}{2}[kC + \frac{1}{2}(1-\nu)\,\Gamma\,(1+C)\,N^2]$$

$$c_{15} = \Gamma$$

$$c_{21} = -NS\,[\frac{1}{2}(3-\nu) + k + \frac{3}{8}(1-\nu)\,\Gamma\,(1+C)^2]$$

$$c_{22} = (1-\nu^2)\,\epsilon^2\lambda - \frac{1}{2}(1-\nu)\,(C+S^2) - N^2 - \frac{1}{2}k\,(N^2+S^2+C^2) - kC - \Gamma N^2 C^2$$
$$+ \frac{1}{8}(1-\nu)\,\Gamma\,(1+3C)\,[S^2\,(5+3C) - C\,(1+3C)]$$

$$c_{23} = N\left\{ -\nu + C + k\,(1+C) + \Gamma N^2 C + \frac{1}{2}(1-\nu)\,\Gamma\,[C\,(1+3C) - 3S^2(1+C)]\right\}$$

$$c_{24} = \Gamma NS\,[C - \frac{1}{2}(1-\nu)]$$

$$c_{31} = S\,[\nu - C - k\,(1+\frac{1}{2}C)]$$

$$c_{32} = -N\left\{ -\nu + C + k\,(1+C) + \Gamma N^2 C - \frac{1}{2}(1-\nu)\,\Gamma\,[S^2 - \frac{1}{2}C\,(1+3C)]\right\}$$

$$c_{33} = -(1-\nu^2)\,\epsilon^2\lambda + 1 - 2\nu C + C^2 + \frac{1}{2}kC\,(3+C) + \frac{1}{2}kN^2 + \Gamma N^4 + (1-\nu)\Gamma N^2 C$$

$$c_{34} = \frac{1}{2}S\,[k + (3-\nu)\,\Gamma\,N^2]$$

$$c_{35} = -\Gamma S$$

$$c_{41} = -1$$

$$c_{44} = 1$$

$$c_{51} = -\frac{1}{4}(1-\nu)(1+C)N^2$$

$$c_{52} = NS\left[C+\nu(1+C)+\frac{1}{4}(1-\nu)(1+3C)\right]$$

$$c_{53} = -2N^2 S$$

$$c_{54} = \nu C - S^2 - \frac{1}{2}(1-\nu)N^2$$

$$c_{55} = -1$$

The coefficients in equation (40) are:

$$\bar{a}_{33} = a_{33} - T_0\, a_{23}$$

$$\bar{b}_{3i} = b_{3i} - T_0\, b_{2i} \qquad i = 1, 2, 3, 4$$

$$\bar{c}_{3i} = c_{3i} - T_0\, c_{2i} \qquad i = 1, 2, 3, 4$$

where

$$T_0 = \frac{\frac{1}{4}(1-\nu)\,\Gamma\,(1+3C)\,N}{\frac{1}{2}(1-\nu)+k\left(1+\frac{1}{2}C\right)+\frac{1}{8}(1-\nu)\,\Gamma\,(1+3C)^2}$$

The elements of the A, B, and C matrices are:

$$A_{11} = Q^2\left[1+k\left(1+\frac{1}{2}C\right)\right]+Q\,T_1\,T_7$$

$$A_{12} = Q\,T_3\,T_7$$

$$A_{13} = Q\,T_5\,T_7$$

$$A_{14} = -\Gamma\,Q\,T_7$$

$$A_{21} = Q\,T_1\,T_9$$

$$A_{22} = Q^2\left[\tfrac{1}{2}(1-\nu) + k\left(1+\tfrac{1}{2}C\right) + \tfrac{1}{8}(1-\nu)\,\Gamma\,(1+3C)^2\right] + Q\,T_3\,T_9$$

$$A_{23} = Q\,T_5\,T_9$$

$$A_{24} = -\Gamma\,Q\,T_9$$

$$A_{31} = Q\,T_1$$

$$A_{32} = Q\,T_3$$

$$A_{33} = Q\,T_5$$

$$A_{34} = -\Gamma\,Q$$

$$A_{41} = Q\,T_1\,T_{11}$$

$$A_{42} = Q\,T_3\,T_{11}$$

$$A_{43} = Q^2 + Q\,T_5\,T_{11}$$

$$A_{44} = -\Gamma\,Q\,T_{11}$$

$$B_{11} = Q^2 S\left(1+\tfrac{1}{2}k\right) + Q\,T_7\,(T_1' + T_2) + T_1\,T_8$$

$$B_{12} = \tfrac{1}{2}Q^2 N\left[(1+\nu) - \tfrac{1}{4}(1-\nu)\,\Gamma\,(1+C)\,(1+3C)\right] + Q\,T_7\,(T_3' + T_4) + T_3\,T_8$$

$$B_{13} = Q\,T_7\,(T_5' + T_6) + T_5\,T_8$$

$$B_{14} = -\Gamma\,(Q\,S\,T_7 + T_8)$$

$$B_{21} = -\tfrac{1}{2}Q^2 N\left[1+\nu+\tfrac{1}{4}(1-\nu)\,\Gamma\,(1+3C)\,(1-C)\right] + Q\,T_9\,(T_1' + T_2) + T_1\,T_{10}$$

$$B_{22} = \tfrac{1}{2}Q^2 S\left[1-\nu-\tfrac{1}{4}(1-\nu)\,\Gamma\,(1+3C)\,(5+3C)\right] + Q\,T_9\,(T_3' + T_4) + T_3\,T_{10}$$

$$B_{23} = \Gamma\,Q^2 N\left[\nu C + \tfrac{1}{2}(1-\nu)\,(1+3C)\right] + Q\,T_9\,(T_5' + T_6) + T_5\,T_{10}$$

$$B_{24} = -\Gamma(QST_9 + T_{10})$$

$$B_{31} = Q(T_1' + T_2) - Q' T_1$$

$$B_{32} = Q(T_3' + T_4) - Q' T_3$$

$$B_{33} = Q(T_5' + T_6) - Q' T_5$$

$$B_{34} = -\Gamma(QS - Q')$$

$$B_{41} = Q T_{11} (T_1' + T_2) + T_1 T_{12}$$

$$B_{42} = -Q^2 N [\nu C + \frac{1}{4}(1-\nu)(1+3C)] + Q T_{11} (T_3' + T_4) + T_3 T_{12}$$

$$B_{43} = Q^2 S + Q T_{11} (T_5' + T_6) + T_5 T_{12}$$

$$B_{44} = -\Gamma(QST_{11} + T_{12})$$

$$C_{11} = Q^2 [(1-\nu^2)\epsilon^2\lambda + \nu C - S^2 - \frac{1}{2}(1-\nu)N^2 - \frac{1}{2}k(N^2+S^2) - \frac{1}{8}(1-\nu)\Gamma(1+C)^2N^2] + Q T_7 T_2' + T_2 T_8$$

$$C_{12} = Q^2 NS [-\frac{1}{2}(3-\nu) - k + \frac{1}{8}(1-\nu)\Gamma(1+C)(1+3C) + QT_7 T_4' + T_4 T_8$$

$$C_{13} = -\frac{1}{2}Q^2 [kC + \frac{1}{2}(1-\nu)\Gamma(1+C)N^2] + QT_7 T_6' + T_6 T_8$$

$$C_{14} = \Gamma[Q^2 - QT_7(C - S^2) - ST_8]$$

$$C_{21} = -Q^2 NS [\frac{1}{2}(3-\nu) + k + \frac{3}{8}(1-\nu)\Gamma(1+C)^2] + QT_9 T_2' + T_2 T_{10}$$

$$C_{22} = Q^2 \Big\{ (1-\nu^2)\epsilon^2\lambda - \frac{1}{2}(1-\nu)(C+S^2) - N^2 - \frac{1}{2}k(N^2+S^2+C^2) - kC - \Gamma N^2 C^2 + \frac{1}{8}(1-\nu)\Gamma(1+3C)[S^2(5+3C) - C(1+3C)]\Big\} + QT_9 T_4' + T_4 T_{10}$$

$$C_{23} = \Gamma Q^2 NS [C - \frac{1}{2}(1-\nu)] + QT_9 T_6' + T_6 T_{10}$$

$$C_{24} = -\Gamma\,[Q T_9 (C - S^2) + S T_{10}]$$

$$C_{31} = -Q^2 + Q T_2' - Q' T_2$$

$$C_{32} = Q T_4' - Q' T_4$$

$$C_{33} = Q^2 + Q T_6' - Q' T_6$$

$$C_{34} = -\Gamma\,[Q (C - S^2) - Q' S]$$

$$C_{41} = -\frac{1}{4}(1-\nu)(1+C) N^2 Q^2 + Q T_{11} T_2' + T_2 T_{12}$$

$$C_{42} = Q^2 N S\,[C + \nu (1+C) + \frac{1}{4}(1-\nu)(1+3C)] + Q T_{11} T_4' + T_4 T_{12}$$

$$C_{43} = Q^2\,[\nu C - S^2 - \frac{1}{2}(1-\nu) N^2] + Q T_{11} T_6' + T_6 T_{12}$$

$$C_{44} = -Q^2 - \Gamma\,[Q T_{11} (C - S^2) + S T_{12}]$$

where

$$T_1 = 1 - \nu C + \frac{1}{2} k C - \frac{1}{4}(1-\nu)\Gamma N^2 (1-C) + \frac{1}{2} N T_0 [1 + \nu + \frac{1}{4}(1-\nu)\Gamma (1+3C)(1-C)]$$

$$T_2 = S\,[\nu - C - k(1 + \frac{1}{2}C) + \frac{1}{2}(1-\nu)\Gamma N^2] + N S T_0 [\frac{1}{2}(3-\nu) + k + \frac{3}{8}(1-\nu)\Gamma (1+C)^2 - \frac{1}{2}(1-\nu)\Gamma (2+3C)]$$

$$T_3 = -\frac{1}{2}(1-\nu)\Gamma N S - \frac{1}{2} S T_0\,[1 - \nu + k + \frac{1}{4}(1-\nu)\Gamma (1+3C)(5+3C)]$$

$$T_4 = N \Big\{ \nu - C - k(1+C) + \Gamma [-N^2 C + \frac{1}{2}(1-\nu) S^2 - \frac{1}{4}(1-\nu)(1+3C)\,C] \Big\} - T_0 \Big\{ (1-\nu^2)\epsilon^2 \lambda - \frac{1}{2}(1-\nu)(C+S^2) - N^2 - \frac{1}{2} k\,(N^2 + S^2 + C^2) - kC - \Gamma N^2 C^2 + \frac{1}{8}(1-\nu)\Gamma (1+3C)[S^2 (5+3C) - C(1+3C)] \Big\}$$

$$T_5 = k\,(1 + \frac{1}{2}C) + \Gamma N^2 - \Gamma N T_0\,[\nu C + \frac{1}{2}(1-\nu)(1+3C)]$$

$$T_6 = S \Big\{ \frac{1}{2} k + \Gamma N^2 + \frac{1}{2}\Gamma N T_0\,[1 - \nu + (1 - 3\nu) C] \Big\}$$

$$T_7 = 1 - \nu C + k\,(1 + \frac{1}{2}C) + \frac{1}{4}(1-\nu)\Gamma (1+C) N^2$$

$$T_8 = QS\,(1+C)\,[1+\tfrac{1}{2}k - \tfrac{1}{2}(1-\nu)\,\Gamma N^2] - Q'\,T_7$$

$$T_9 = \tfrac{1}{2}(1-\nu)\Gamma\,NS\,(2+3C)$$

$$T_{10} = QN\,[-\nu+C+k\,(1+C) + \Gamma N^2 C + \tfrac{1}{2}(1-\nu)\Gamma\,(1+3C)(C-2S^2)$$
$$- \tfrac{1}{2}(1-\nu)\Gamma\,(1-3C)\,S^2] - Q'\,T_9$$

$$T_{11} = \tfrac{1}{2}(1+\nu)\,N^2$$

$$T_{12} = -(2N^2 SQ + Q'\,T_{11})$$

and prime indicates differentiation with respect to α. In differentiating N, S, and C the following formulas are useful:

$$N' = -NS$$

$$S' = C - S^2$$

$$C' = -S\,(1+C)$$

APPENDIX B

Flexural Vibration of the Prestressed Circular Ring

The vibrations of a circular ring of radius R, prestressed by pressure p, may be determined from equations (15-21) and (24-37) by setting $\epsilon = \nu = v = S_\theta = 0$. This results in the following equations:

Equilibrium

$$N_\alpha' + \frac{1}{R} Q_\alpha + S_\alpha (E_\alpha' - \phi_\alpha) + pR\phi_\alpha + \rho h R^2 \omega^2 u = 0 \qquad \text{(B1)}$$

$$N_\alpha - \frac{1}{R} Q_\alpha' + S_\alpha (\phi_\alpha' + E_\alpha) - pRE_\alpha - \rho h R^2 \omega^2 w = 0 \qquad \text{(B2)}$$

$$M_\alpha' - \frac{1}{R} Q_\alpha = 0 \qquad \text{(B3)}$$

Strain Displacement

$$E_\alpha = u' + w \qquad \text{(B4)}$$

$$R\kappa_\alpha = \phi_\alpha' \qquad \text{(B5)}$$

$$\phi_\alpha = - w' + u \qquad \text{(B6)}$$

Constitutive Relations

$$N_\alpha = Eh E_\alpha \qquad \text{(B7)}$$

$$M_\alpha = \frac{Eh^3}{12} \kappa_\alpha \qquad \text{(B8)}$$

Prestress

$$S_\alpha = pR \qquad \text{(B9)}$$

Substitution of (B3-B9) into B1 and B2 yields

$$(1 + \kappa + \Gamma) u'' + \epsilon^2 \lambda u - \Gamma w''' + (1 + \kappa) w' = 0 \qquad \text{(B10)}$$

$$- \Gamma u''' + (1 + \kappa) u' + \Gamma w'''' - \kappa w'' + (1 - \epsilon^2 \lambda) w = 0 \qquad \text{(B11)}$$

which with

$$u = a_m \sin m\alpha \tag{B12}$$

$$w = b_m \cos m\alpha \tag{B13}$$

yields the following frequency equation

$$(\epsilon^2\lambda)^2 - [1 + m^2 + 2\kappa m^2 + \Gamma m^2 (1 + m^2)] (\epsilon^2\lambda) + m^2 (m^2 - 1) [\kappa (1 + \kappa) + \kappa\Gamma m^2 + \Gamma(m^2 - 1)] = 0 \tag{B14}$$

For $\kappa << 1$ and m not large the lowest root of this frequency equation is approximately

$$\lambda \approx \frac{1}{\epsilon^2} \frac{m^2(m^2 - 1)}{m^2 + 1} [\kappa + \Gamma(m^2 - 1)] \tag{B15}$$

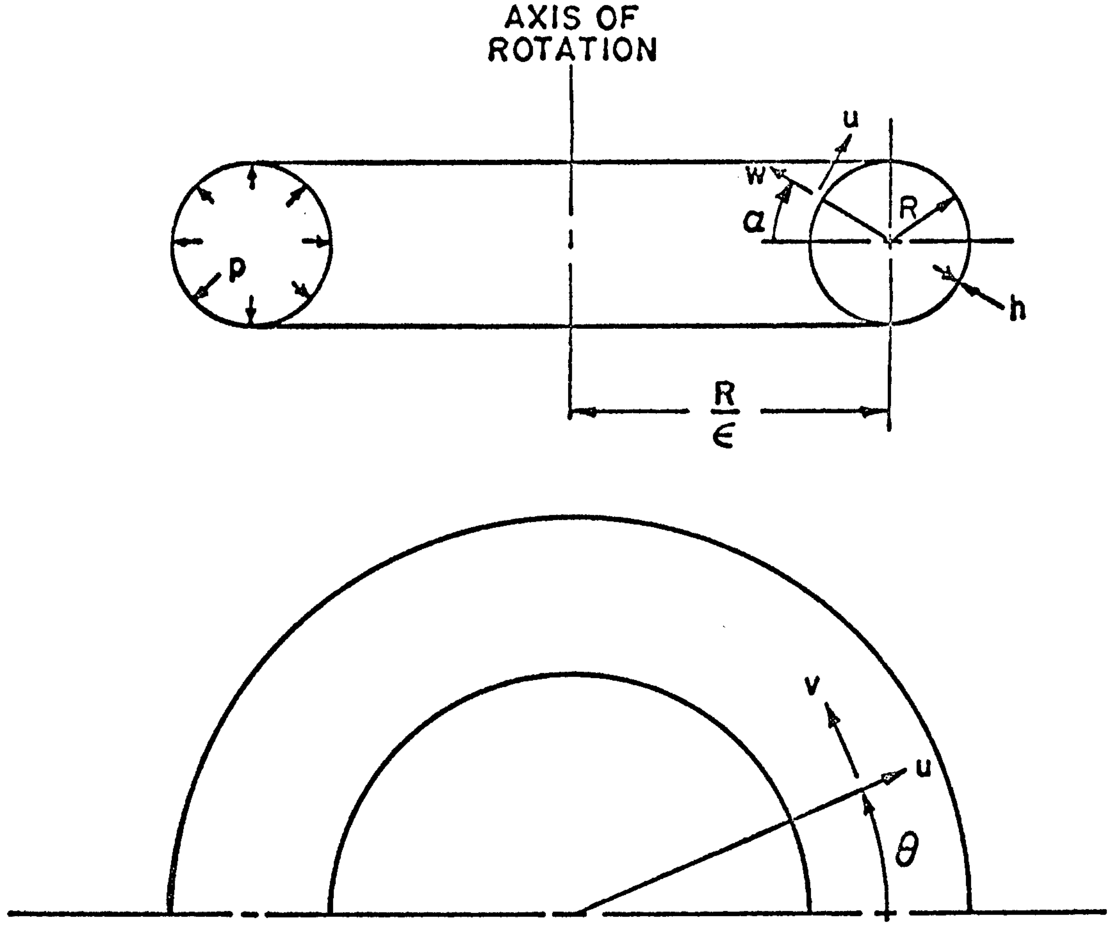

FIGURE 1: GEOMETRY AND NOTATION

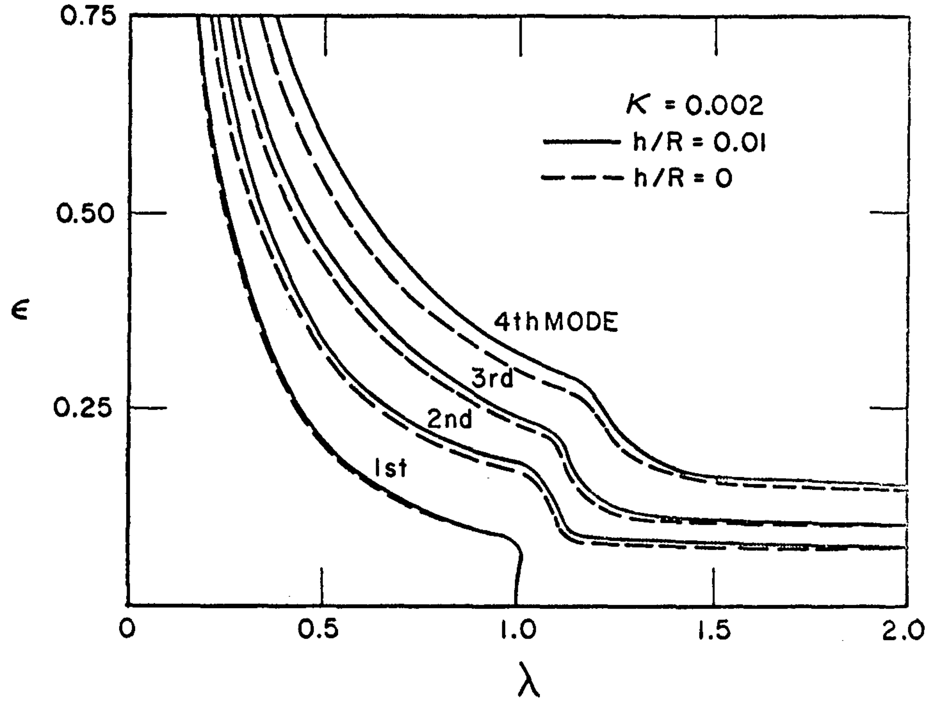

FIG. 2: AXISYMMETRIC MODES, SYMMETRIC, $\kappa = 0.002$

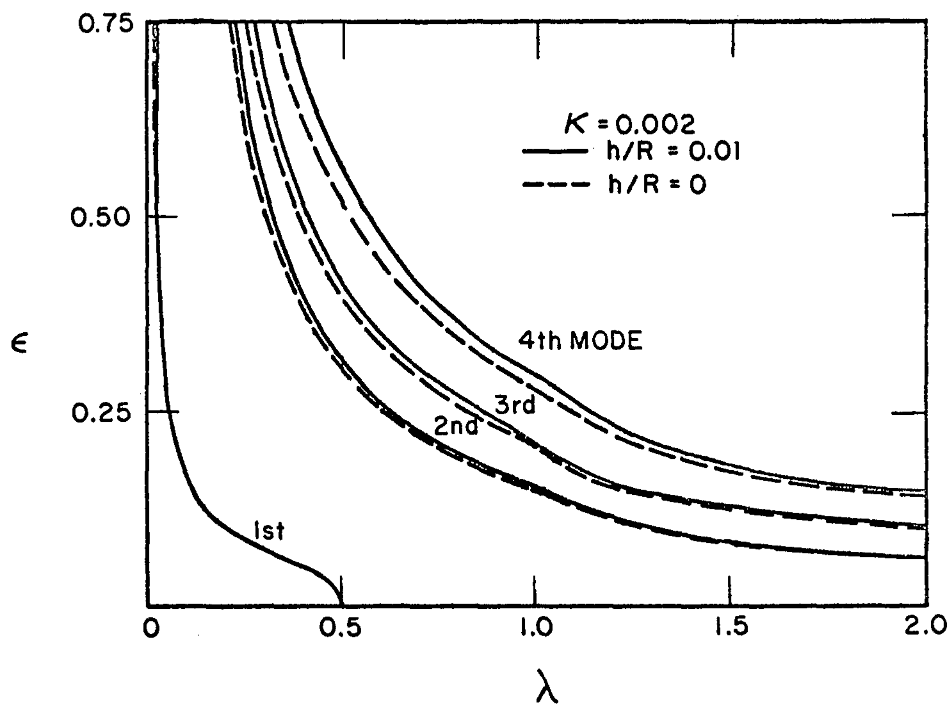

FIG. 3: AXISYMMETRIC MODES, ANTISYMMETRIC, $\kappa = 0.002$

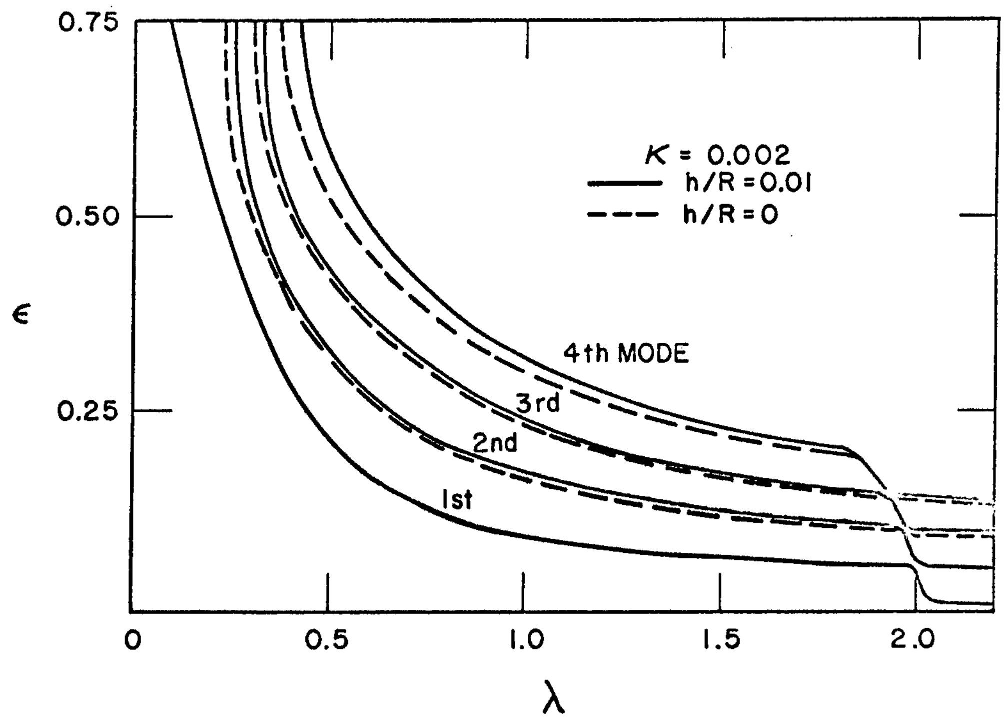

FIG. 4: n = I MODES, SYMMETRIC, K = 0.002

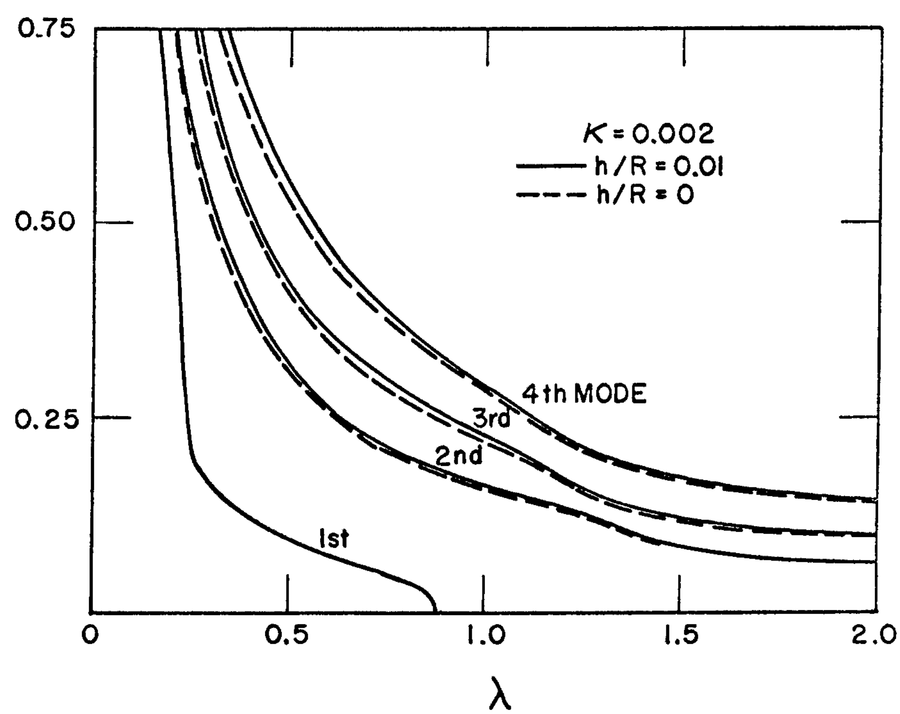

FIG. 5: n = I MODES, ANTISYMMETRIC, K = 0.002

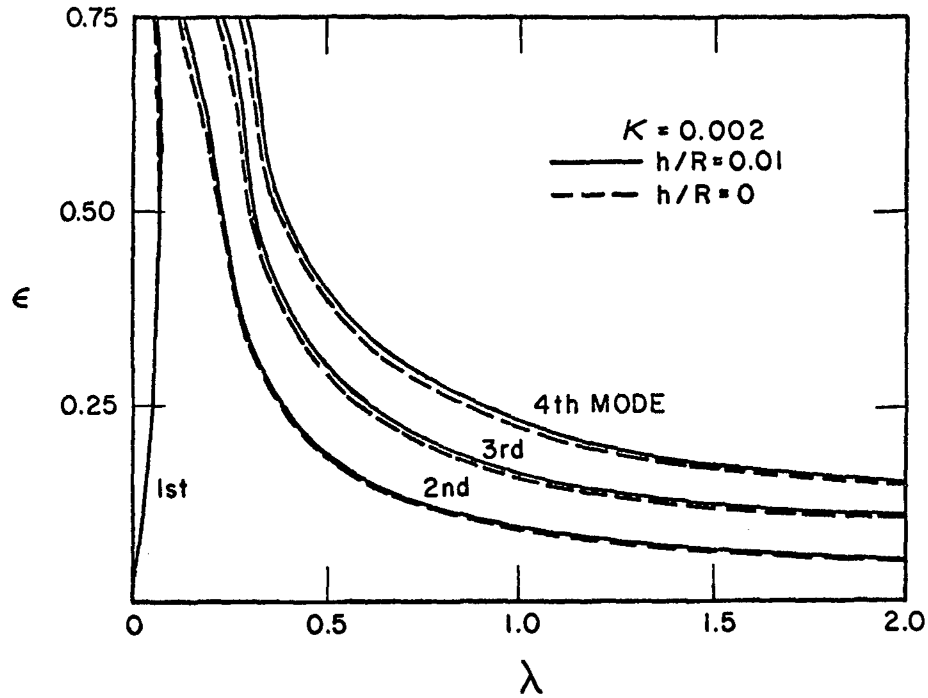

FIG. 6: n = 2 MODES, SYMMETRIC, κ = 0.002

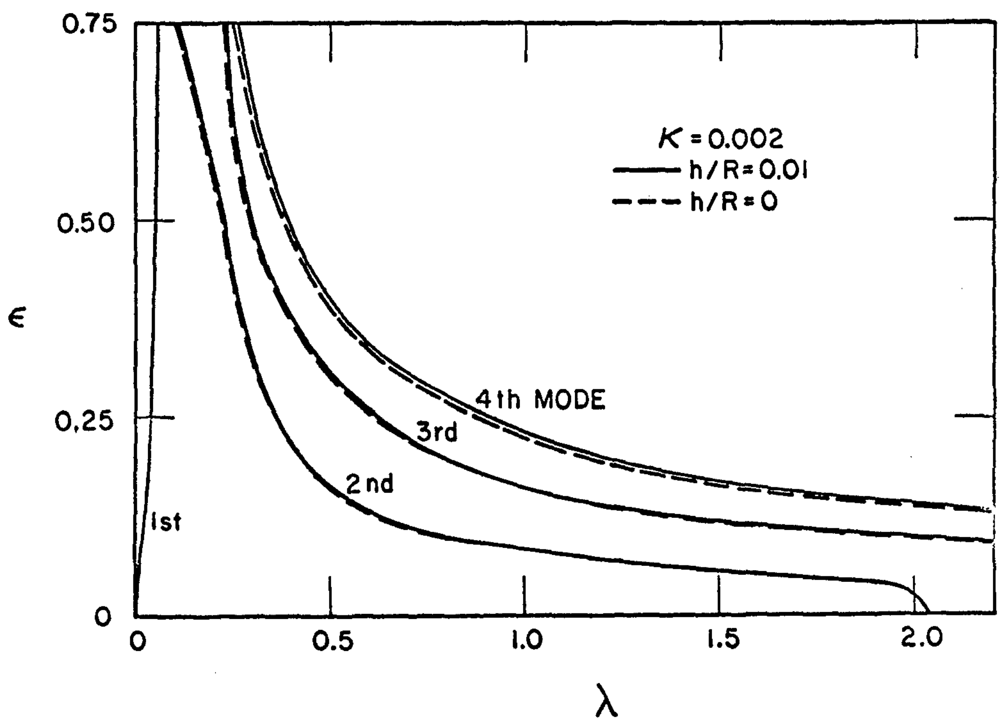

FIG. 7: n = 2 MODES, ANTISYMMETRIC, κ = 0.002

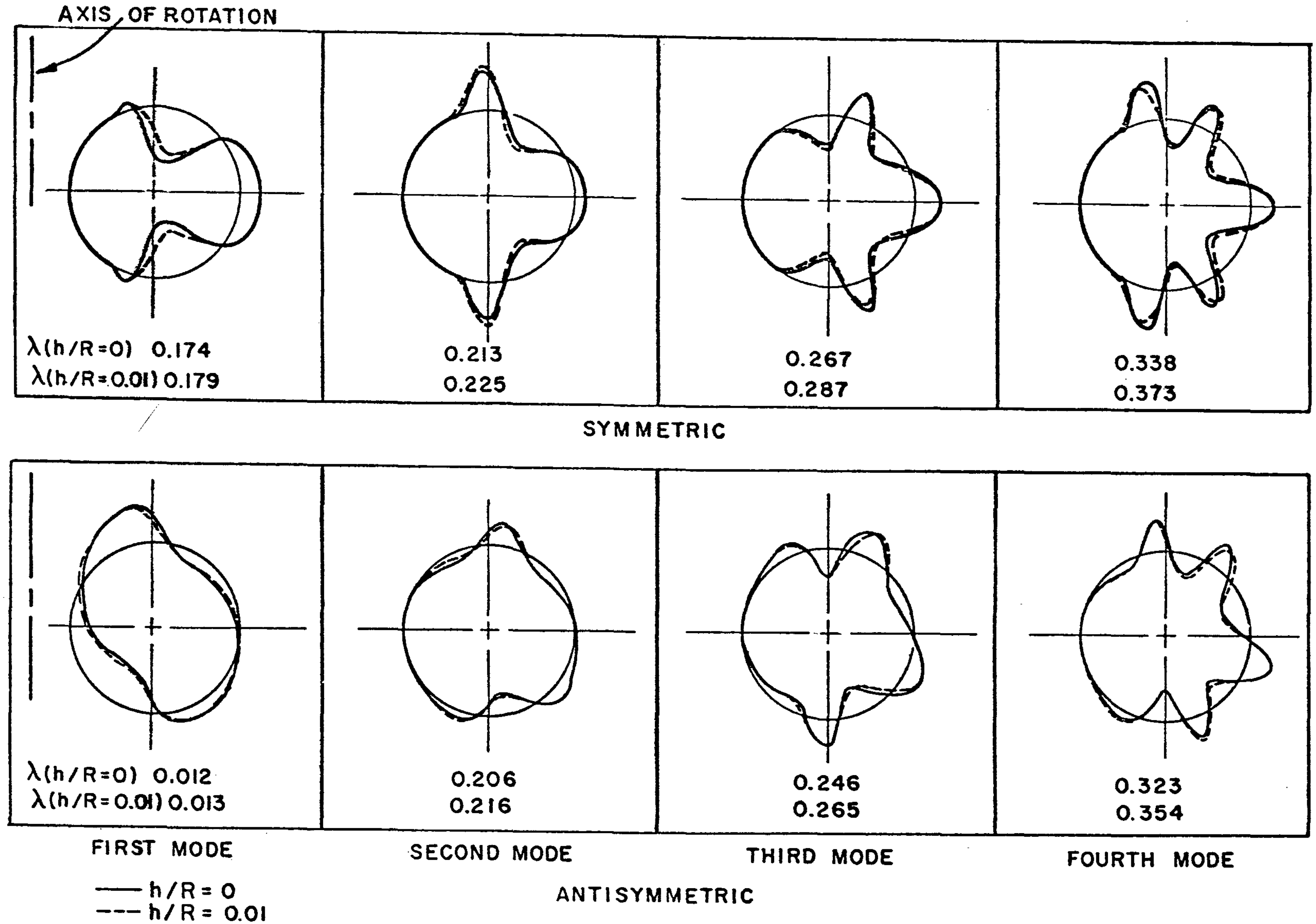

FIG. 8: EFFECT OF BENDING STIFFNESS ON MODE SHAPES, $n=0$, $\kappa=0.002$, $\epsilon=0.75$

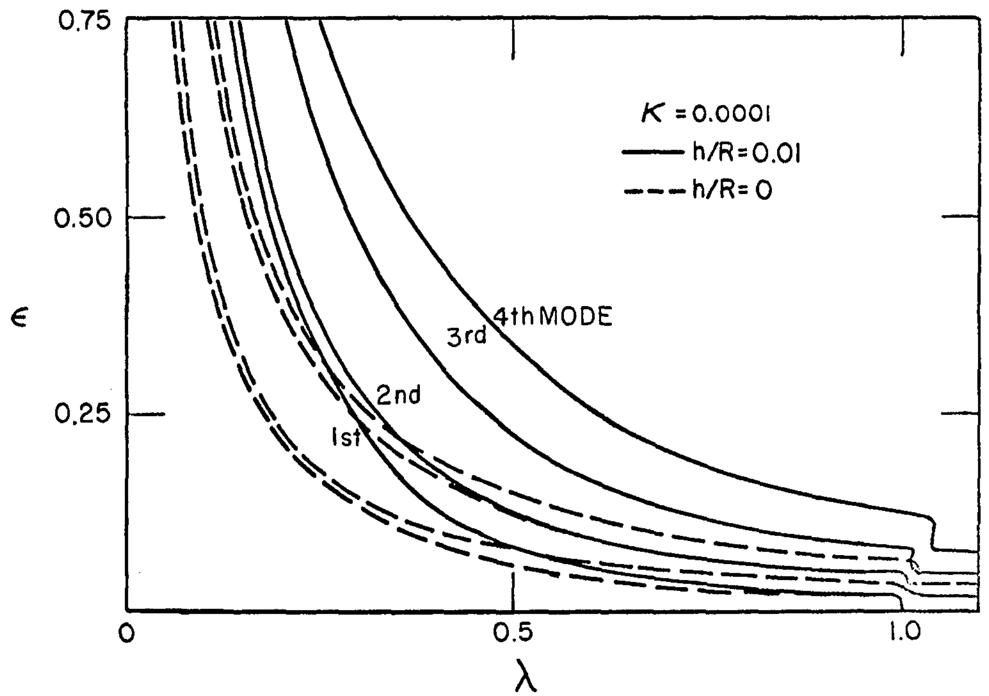

FIG. 9: AXISYMMETRIC MODES, SYMMETRIC, κ = 0.0001

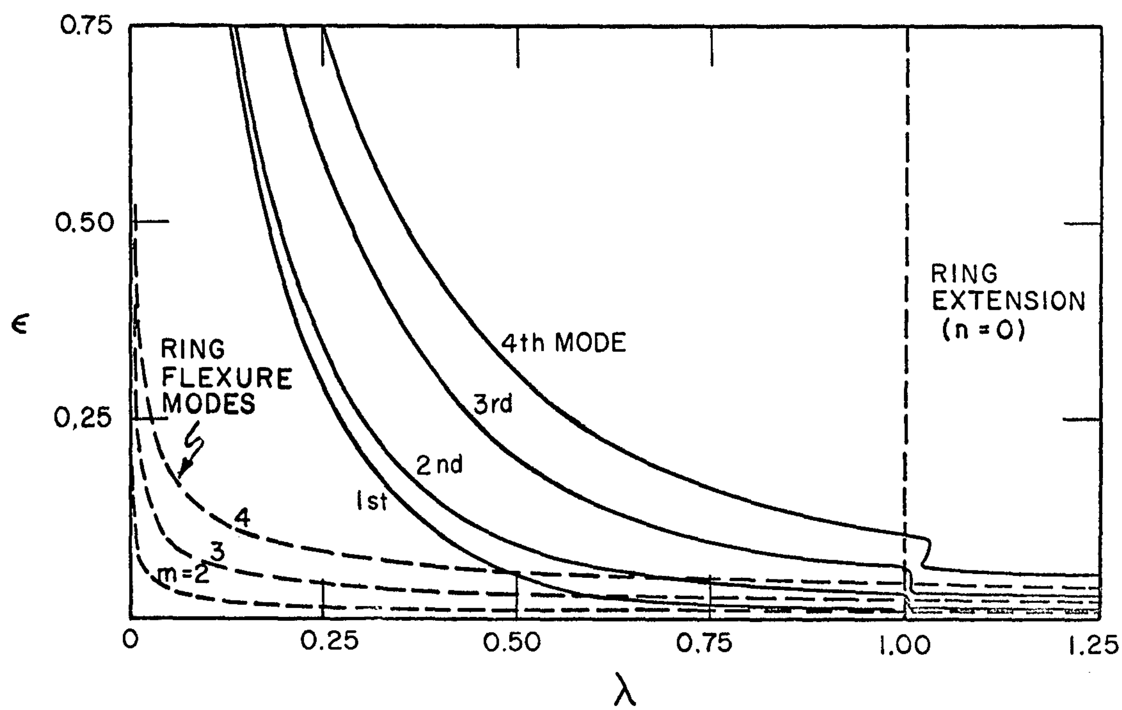

FIG.10: AXISYMMETRIC MODES, SYMMETRIC, κ = 0, h/R = 0.01

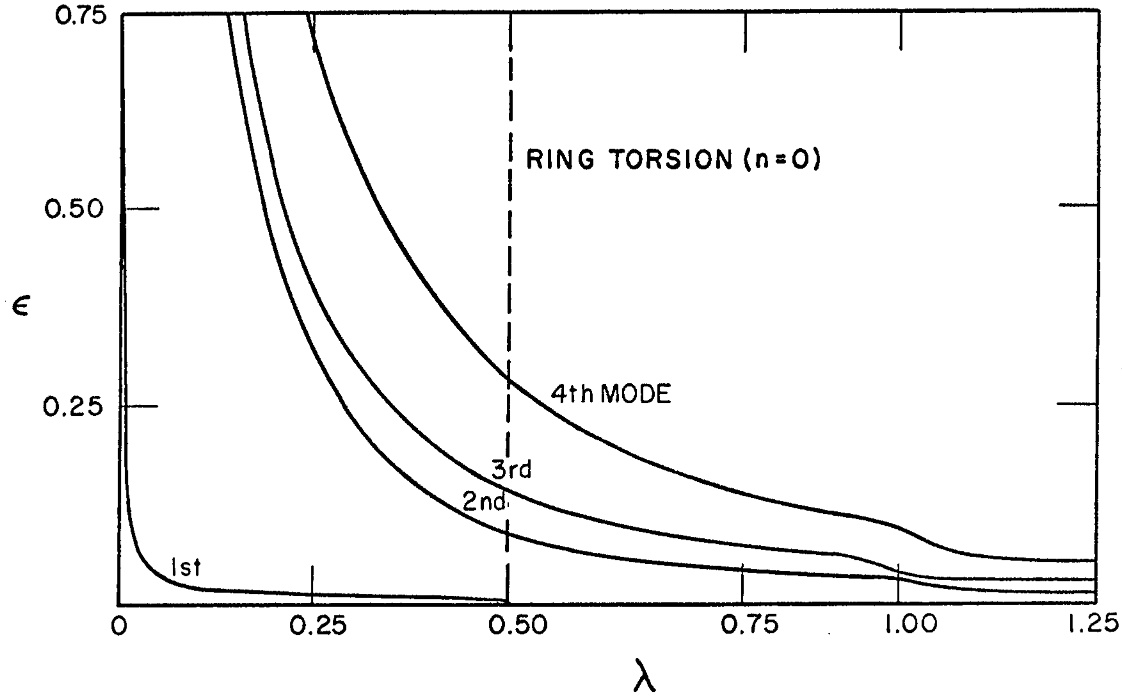

FIG. 11: AXISYMMETRIC MODES, ANTISYMMETRIC, $\kappa=0$, $h/R=0.01$

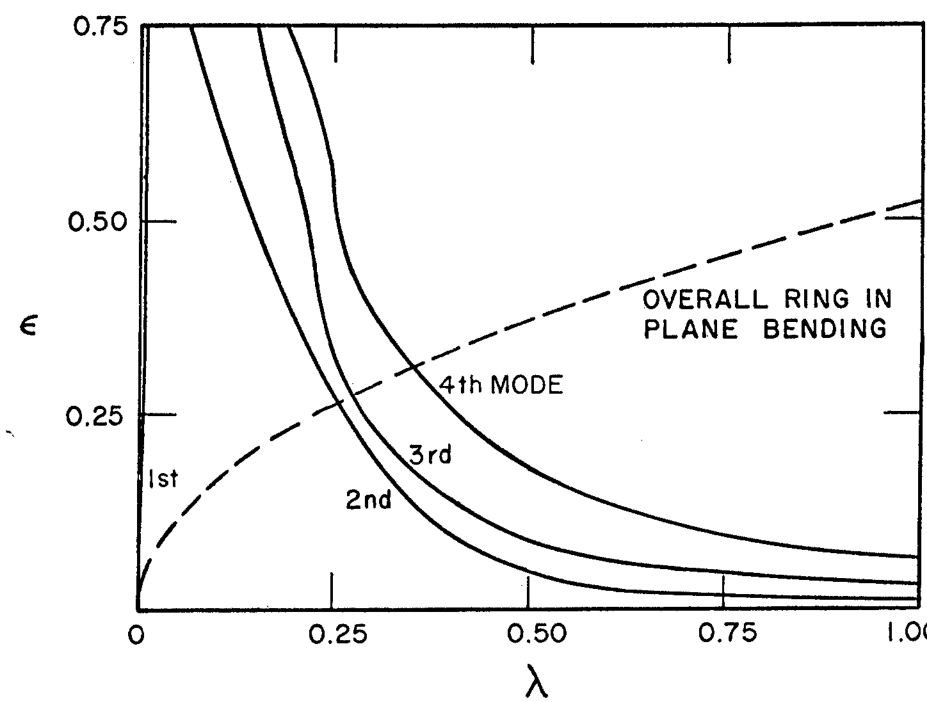

FIG. 12: $n=2$ MODES, SYMMETRIC, $\kappa=0$, $h/R=0.01$

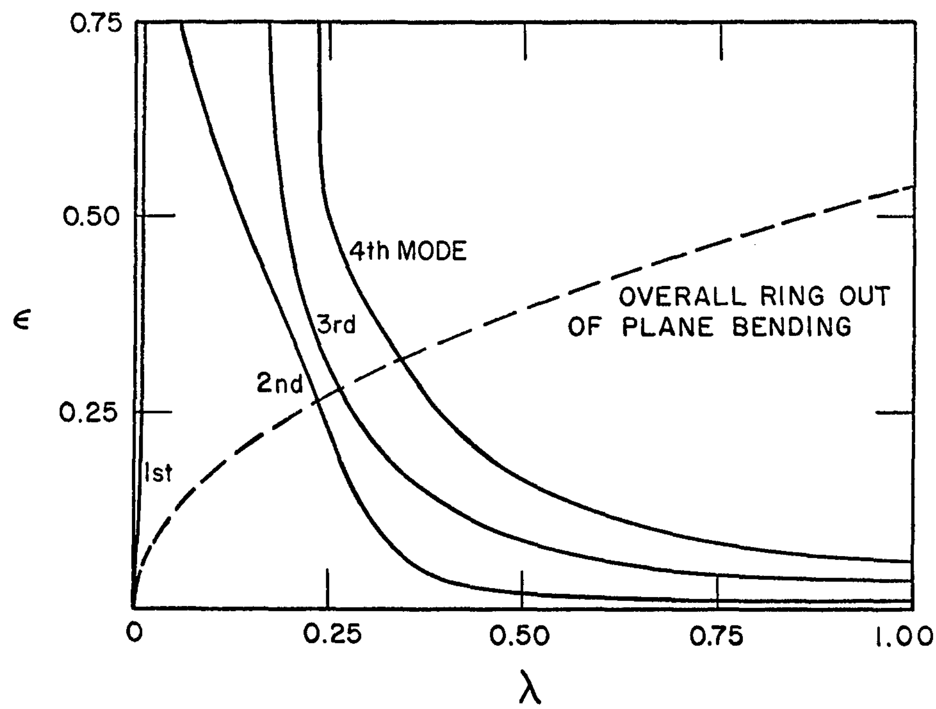

FIG. 13: n = 2 MODES, ANTISYMMETRIC, $\kappa = 0$, $h/R = 0.01$

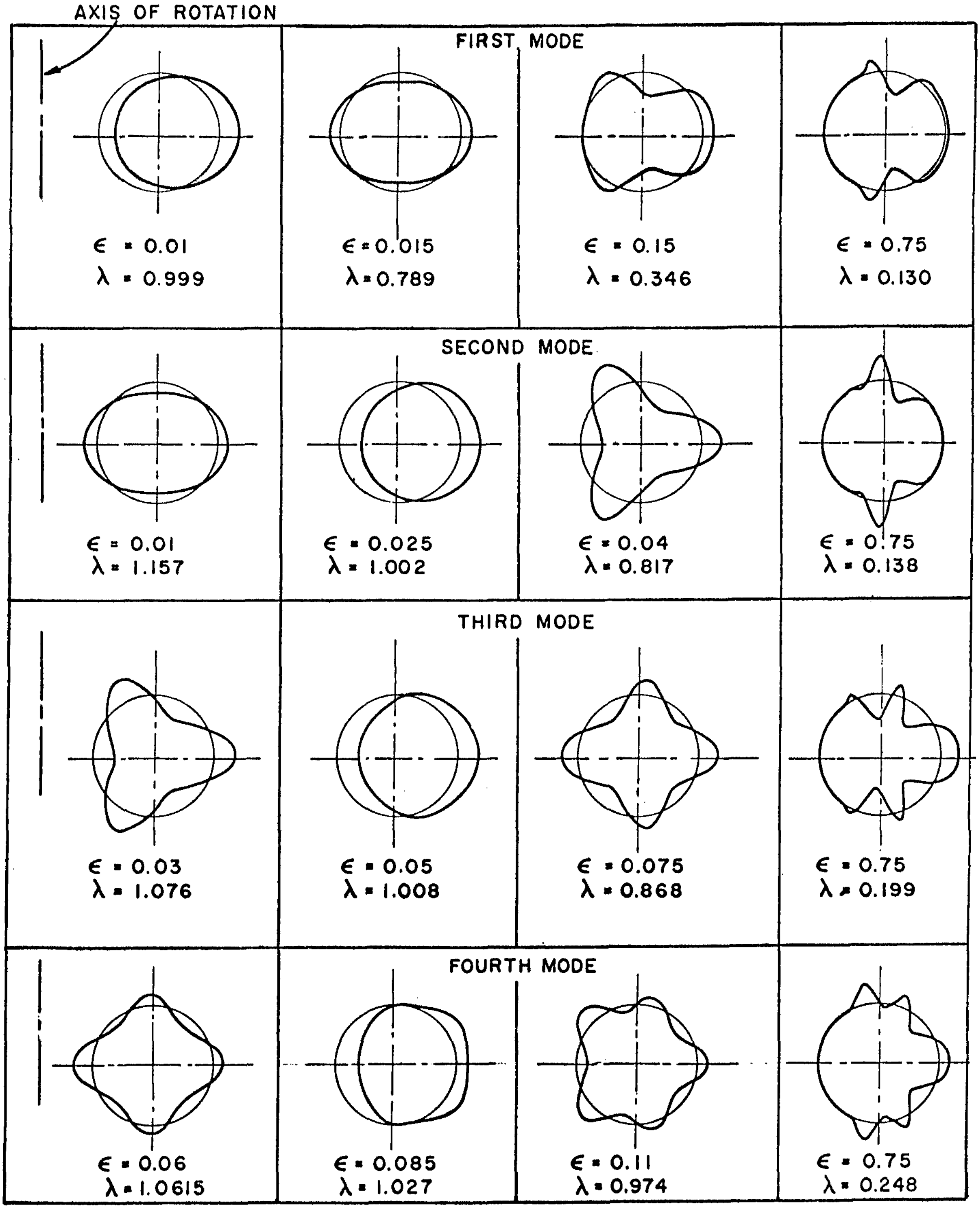

FIG. 14: AXISYMMETRIC MODE SHAPES, SYMMETRIC, $\kappa = 0$, $h/R = 0.01$

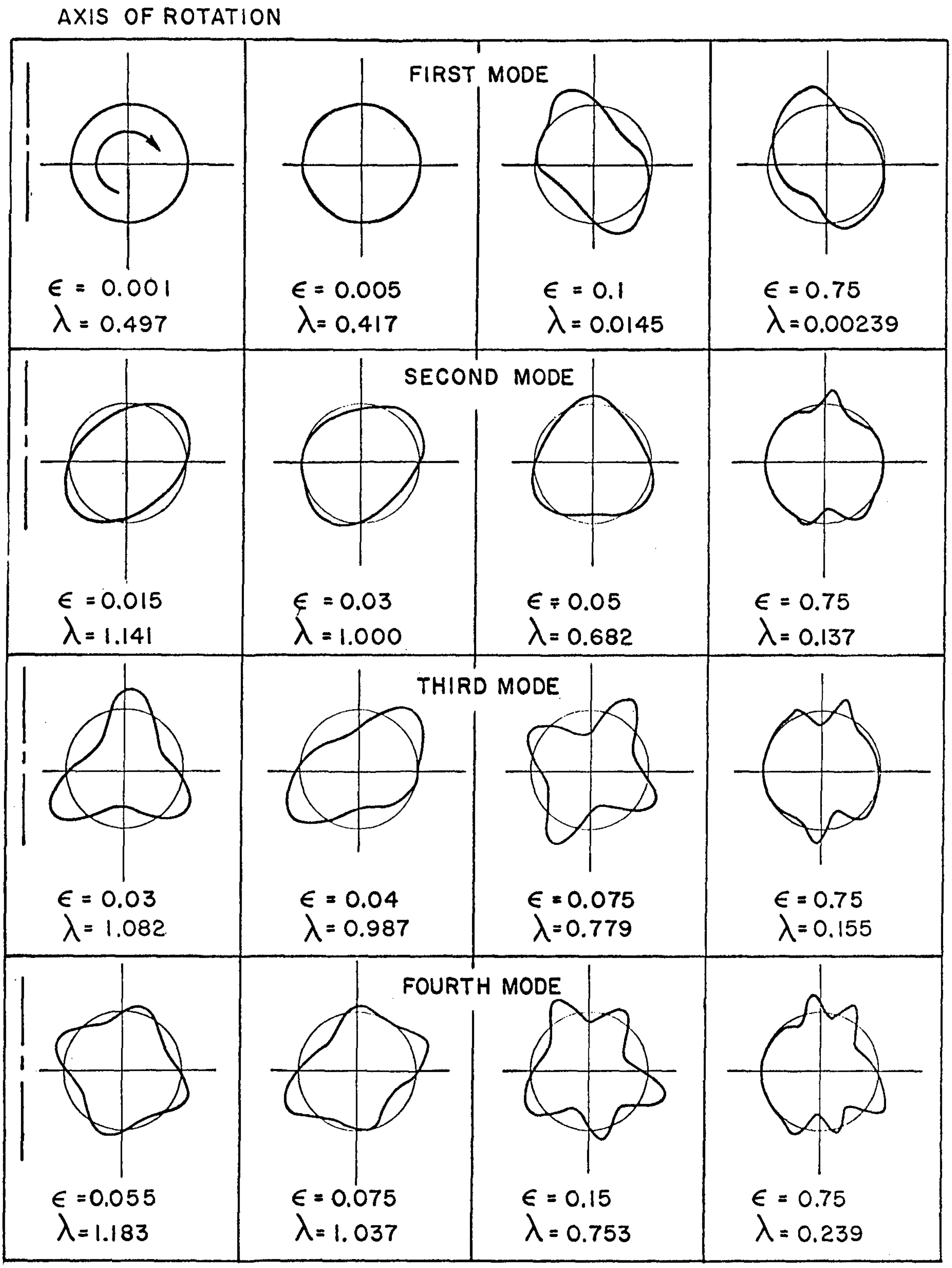

FIG. 15: AXISYMMETRIC MODE SHAPES, ANTISYMMETRIC, κ=0, h/R=0.01

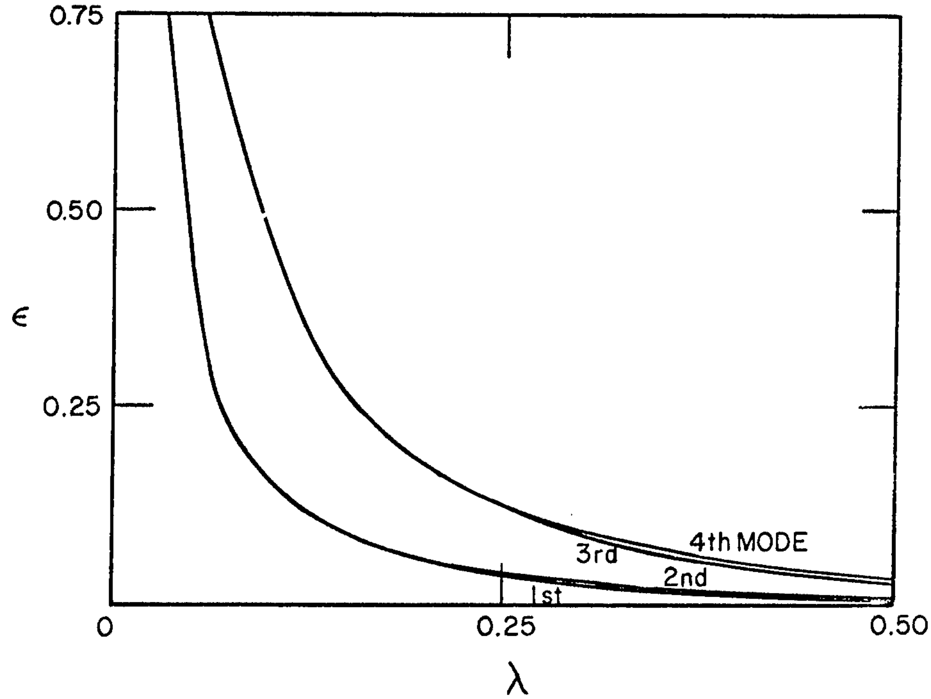

FIG. 16: AXISYMMETRIC MODES, SYMMETRIC, $\kappa=0$, $h/R=0.001$

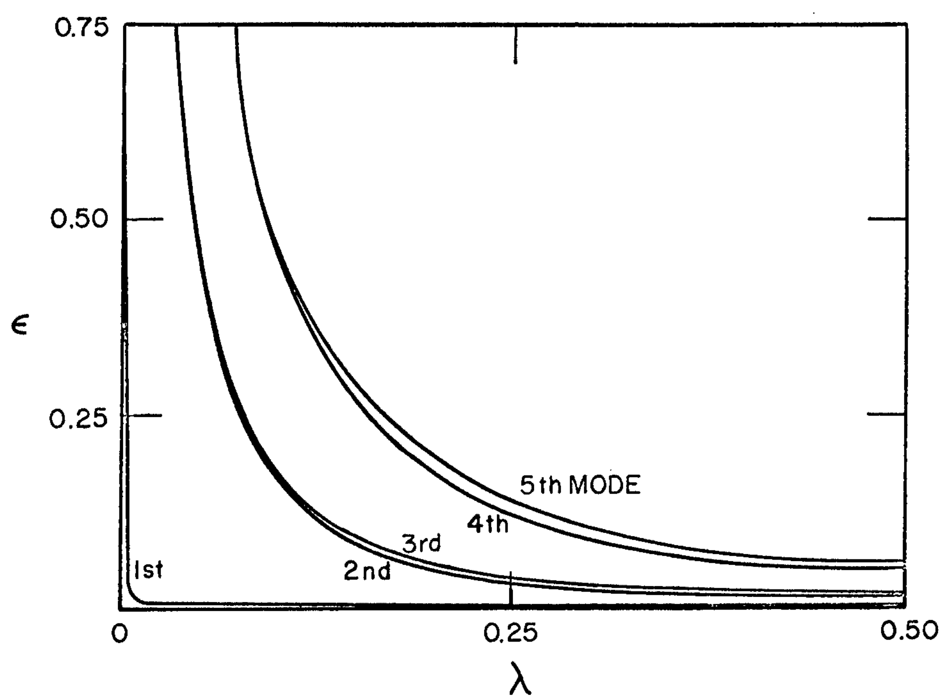

FIG. 17: AXISYMMETRIC MODES, ANTISYMMETRIC, $\kappa=0$, $h/R=0.001$

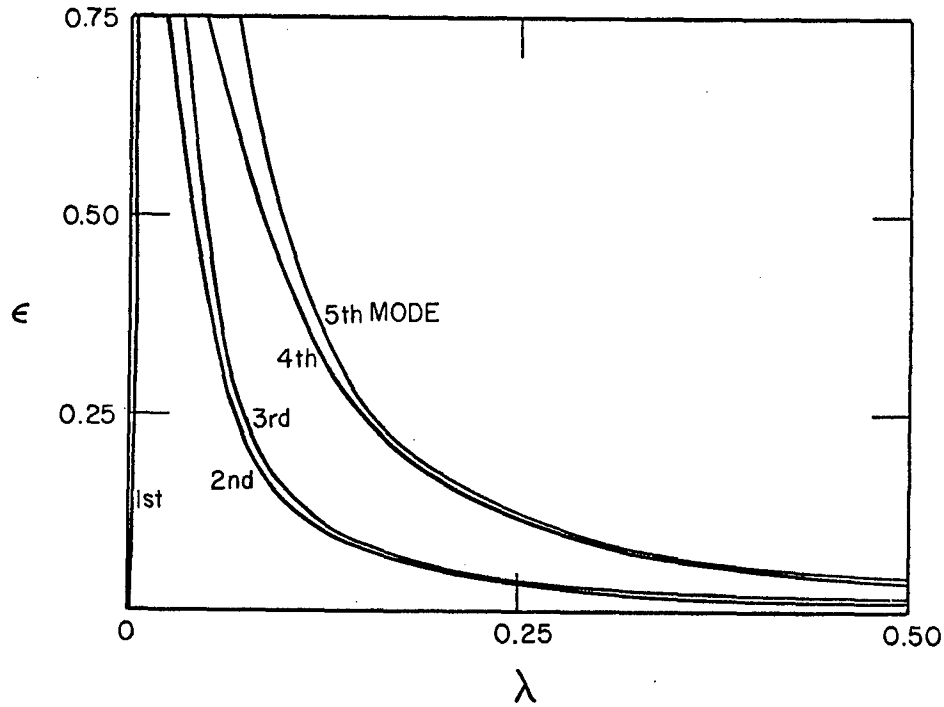

FIG.18: n=2 MODES, SYMMETRIC, κ = 0, h/R = 0.001

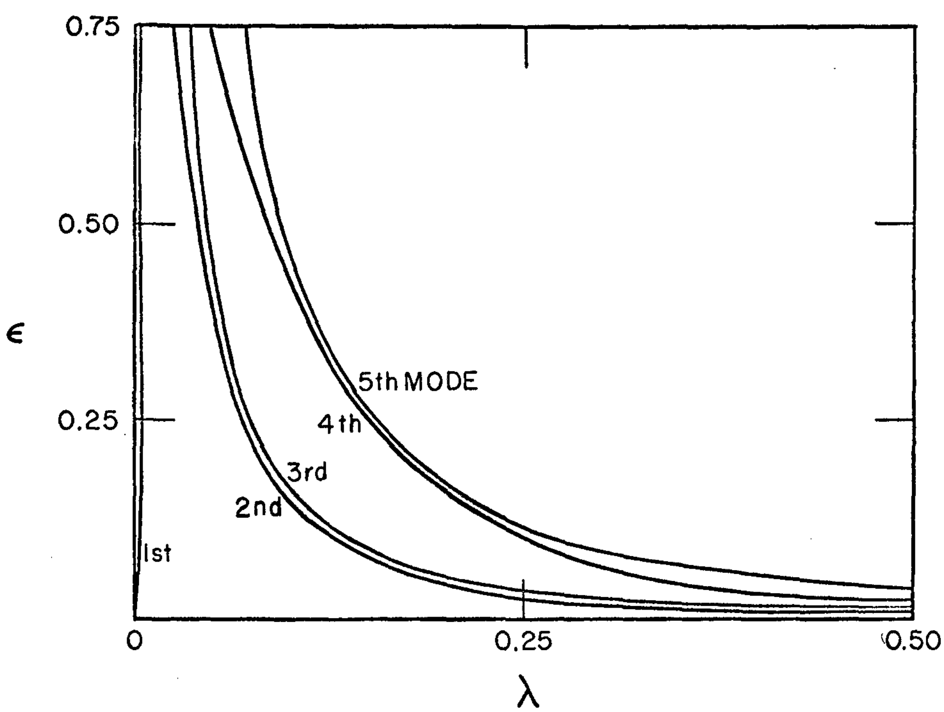

FIG.19: n = 2 MODES, ANTISYMMETRIC, κ = 0, h/R = 0.001

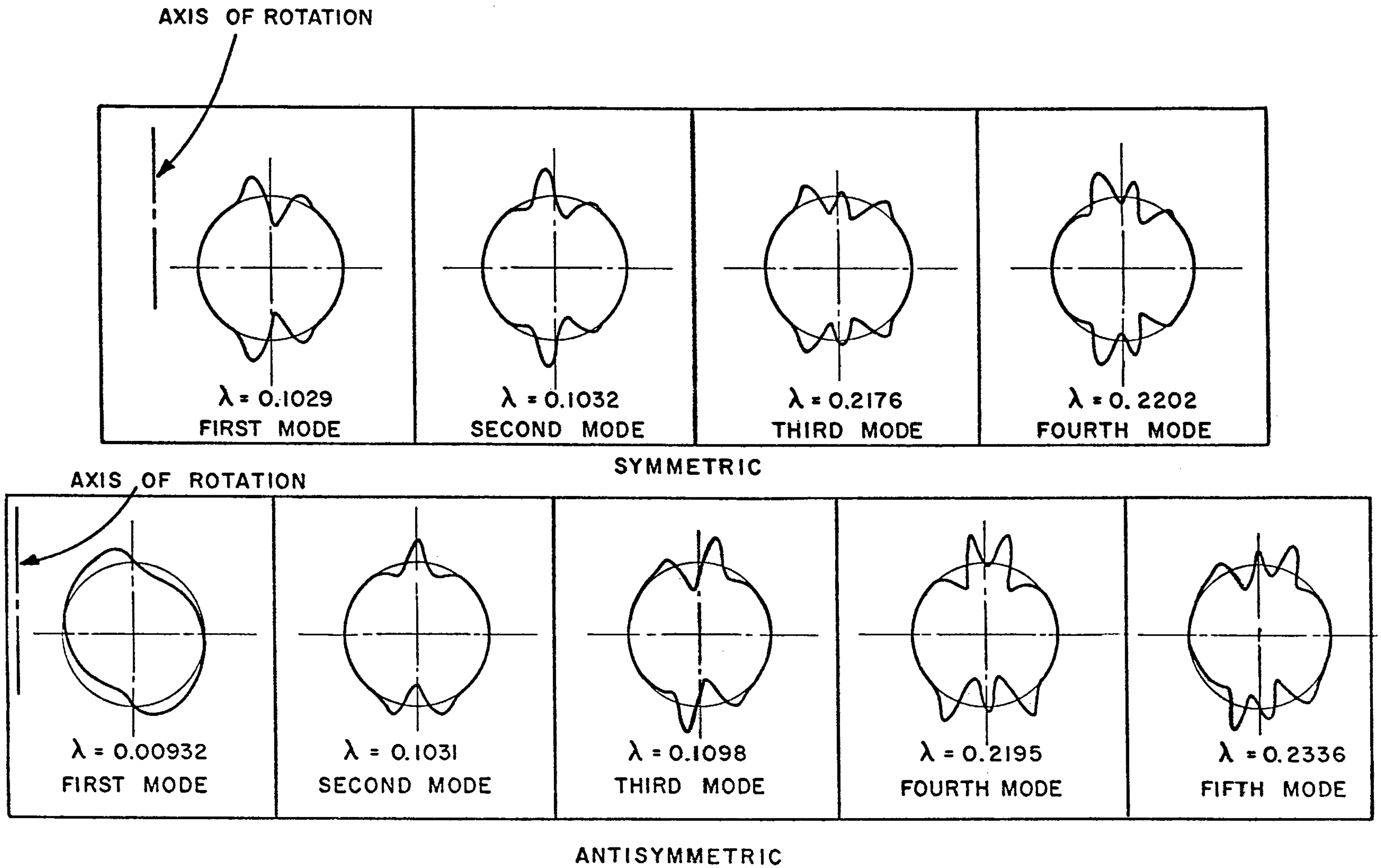

FIG. 20: AXISYMMETRIC MODE SHAPES, $\kappa = 0$, $h/R = 0.001$, $\epsilon = 0.15$

NASA-Langley, 1965 CR-296